Scattering in Mixed Dimensions with Ultracold Gases

G. Lamporesi,[1] J. Catani,[1,2] G. Barontini,[1] Y. Nishida,[3] M. Inguscio,[1,2] and F. Minardi[1,2]

[1]*LENS—European Laboratory for Nonlinear Spectroscopy and Dipartimento di Fisica, Università di Firenze, via Nello Carrara 1, I-50019 Sesto Fiorentino, Italy*

[2]*Istituto Nazionale di Ottica (INO)-CNR, via Giovanni Sansone 1, I-50019 Sesto Fiorentino, Italy*

[3]*Center for Theoretical Physics, Massachusetts Institute of Technology, Cambridge, Massachusetts 02139, USA*

(Received 26 January 2010; published 14 April 2010)

We experimentally investigate the mix-dimensional scattering occurring when the collisional partners live in different dimensions. We employ a binary mixture of ultracold atoms and exploit a species-selective 1D optical lattice to confine only one atomic species in 2D. By applying an external magnetic field in proximity of a Feshbach resonance, we adjust the free-space scattering length to observe a series of resonances in mixed dimensions. By monitoring 3-body inelastic losses, we measure the magnetic field values corresponding to the mix-dimensional scattering resonances and find a good agreement with the theoretical predictions based on simple energy considerations.

DOI: 10.1103/PhysRevLett.104.153202 PACS numbers: 34.50.−s, 03.65.Nk, 37.10.Jk, 67.85.−d

Degenerate atomic gases have provided quantum systems with unprecedented possibilities of manipulation and control, achieved by combining magnetic and optical potentials as well as scattering resonances. The capability to model and control tightly confining potentials sparked the experimental investigation on quantum systems of reduced dimensionality, since particles can be forced to occupy a single quantum level along specific directions. Spectacular achievements, such as the observation of the Berezinskii-Kosterlitz-Thouless crossover [1] in 2D and the realization of Tonks-Girardeau gases [2] in 1D, confirmed the importance of quantum gases as test bench for fundamental low-energy physical phenomena. Moreover, low dimensional ultracold atomic gases show further peculiar scattering properties leading to the appearance of confinement-induced resonances (CIR) depending on the dimensionality of the system [3–6]. Interestingly, while much of the work done so far deals with well-defined dimensionality, systems composed of interacting parts living in different dimensions have received little attention and, besides recent theoretical analysis [7,8], experimental investigation is still lacking. Such mix-dimensional systems are relevant in several physical domains, ranging from cosmology to condensed matter physics. In brane theory, for example, particles and fields are confined to the ordinary 3D space and interact with gravitons that can propagate in extra dimensions [9].

In this Letter, we report on the first experimental realization of a mix-dimensional system composed of two ultracold atomic species, ^{41}K and ^{87}Rb, of which we control the mutual interactions. We exploit the technique of species-selective dipole potential (SSDP) proposed in Refs. [7,10] and implemented in Ref. [11], to realize a tight potential confining one species in 2D (^{41}K), while having a negligible effect on the other (^{87}Rb), that remains 3D. In this configuration, for the first time we observe a series of up to 5 scattering resonances, induced by the mixed dimensionality. These discrete resonances are peculiar to configurations having only one collisional partner tightly confined: they are indiscernible in 3D homogeneous (or weakly confined) systems and absent for confined particles with equal harmonic frequencies. Important physical insight about mix-dimensional resonances (MDRs) can be gained by the following simple picture. In general, a scattering resonance may occur when the energy of a closed-channel state equals the energy of scattering partners. For tightly confined atoms, the energy shifts of both the scattering threshold (unbound atoms) and

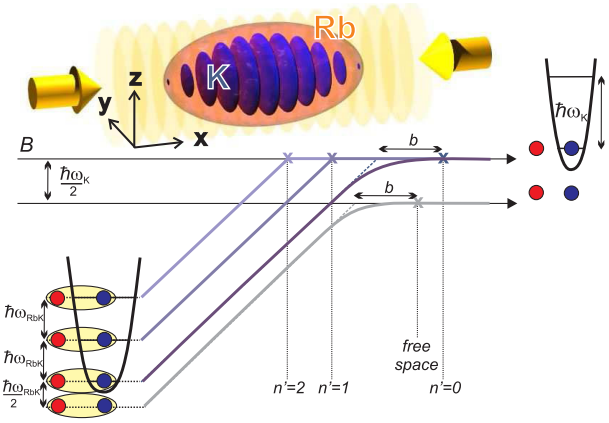

FIG. 1 (color online). (top) Sketch of the experimental configuration: 3D(Rb)-2D(K) mix-dimensional system obtained using a SSDP lattice. (bottom) Energy diagram of the open and closed channel as a function of the Feshbach field B: due to the external potential, both channels are uplifted and split into many levels, separated by the relevant harmonic oscillator quanta $\hbar\omega_i$ (i = K, KRb). MDR may occur when closed-channel levels (n', sloping lines) intercept populated open-channel levels (horizontal lines). The shift b due to the channel coupling is assumed equal to that in free space for $n' = 0$, and is neglected for $n' > 0$.

 © 2010 The American Physical Society

the closed-channel levels (dimer) cannot be neglected. In a collision between an atom A lying in the harmonic ground level along the confined direction x and a free atom B with negligible momentum, resonances might arise when

$$\frac{\hbar\omega}{2} = \hbar\omega\sqrt{\frac{m_A}{m_A + m_B}}\left(n' + \frac{1}{2}\right) - E_b \qquad n' = 0, 1, 2, \ldots, \tag{1}$$

where ω denotes the harmonic frequency of particle A and E_b the free-space binding energy of the (bare) closed channel. Channel coupling, neglected in Eq. (1), causes a resonance position shift b, assumed to be relevant only for $n' = 0$. The series of resonances is absent if the colliding atoms have equal harmonic frequencies because, in this case, the center-of-mass and the internal motion are decoupled and collisions cannot change the center-of-mass energy. In the following, a collection of tight harmonic traps along one direction is provided by a 1D SSDP optical lattice (Fig. 1), such that the harmonic frequency ω of the confined K sample depends on the lattice strength $V_{\rm lat}^{\rm K}$, hereafter expressed in units of K recoil energy [$V_{\rm lat} = s(\hbar k_L)^2/(2m_{\rm K}) = sh \times 7.797$ kHz].

The formal theory of scattering confirms the simple picture above and allows us to derive the scattering amplitude, as well as to define an effective scattering length $a_{\rm eff}$. Here we summarize our analysis following Refs. [7,8], and introducing an effective-range correction that provides an improved approximation for the binding energy beyond the universal region $E_b \propto (1/a^2)$, a being the free-space scattering length.

We consider atoms A and B interacting through a short-range potential $V(\mathbf{r}_A - \mathbf{r}_B)$. Because of translational symmetry, we can separate the center-of-mass motion in the yz plane. The Schrödinger equation reads

$$[H_0 + V - E]\psi(x_A, x_B, \boldsymbol{\rho}_{AB}) = 0,$$

$$H_0 = -\frac{\hbar^2\partial_{x_A}^2}{2m_A} - \frac{\hbar^2\partial_{x_B}^2}{2m_B} - \frac{\hbar^2\nabla_{\boldsymbol{\rho}_{AB}}^2}{2\mu} + \frac{1}{2}m_A\omega^2 x_A^2,$$

where $\boldsymbol{\rho}_{AB} = (y_A - y_B, z_A - z_B)$ and μ is the reduced mass. At short distances $r = \sqrt{(x_A - x_B)^2 + \boldsymbol{\rho}_{AB}^2} \to 0$, the presence of the confining potential is irrelevant and we can replace the real potential V with the generalized Bethe-Peierls boundary condition imposed on the wave function: $\psi|_{r\to 0} \propto 1/r - 1/\tilde{a}(E_c)$, where $\tilde{a}(E_c)^{-1} = a^{-1} - \mu r_0 E_c/\hbar^2$ with E_c denoting the collision energy [12]. On the other hand, the behavior of the zero energy wave function at large distances $r \to \infty$ defines an effective scattering length $a_{\rm eff}$: $\psi|_{E\to(\hbar\omega/2), r\to\infty} \propto [1/\sqrt{\frac{m_B}{\mu}x_B^2 + \boldsymbol{\rho}_{AB}^2} - 1/a_{\rm eff}]e^{-x_A^2/(2l_{\rm ho}^2)}$ [8].

The numerically computed $a_{\rm eff}$ is plotted in Fig. 2(a) for the mass values of our experiment ($A = {}^{41}$K, $B = {}^{87}$Rb), the effective range $r_0 = 168.37a_0$, and the confinement length $l_{\rm ho} = \sqrt{\hbar/m_A\omega} = 1124a_0$. We see that $a_{\rm eff}$ diverges for one particular negative value of a and for an infinite series of positive values of a. The width of successive resonances decreases and, for $l_{\rm ho}/|a| \gg 1$, $a_{\rm eff}$ approaches $a\sqrt{m_B/\mu}$. We also see that the resonant a values coincide with those calculated by using Eq. (1). The theoretical predictions outlined in Fig. 2, combined with the knowledge of the magnetic field dependence of the scattering length in free space, allow for quantitative predictions of the MDRs positions as well as the behavior of $a_{\rm eff}(B)$ [Fig. 2(b)].

In free space, two Feshbach resonances located at 3.84 and 7.87 mT are useful to tune the interspecies scattering length [13]. The binding energies of the weakly bound Feshbach ^{41}K^{87}Rb dimers have been measured [14] and used to adjust the collisional model [15]. For the weakly bound dimer state arising at 3.84 mT, the numerically calculated scattering length as a function of the magnetic field B, in mT, is well reproduced by the parametrization $a(B) = 208a_0(1 + 3.09/(B + 3.852) - 4.992/(B - 3.837) - 0.164/(B - 7.867))$, while the calculated dimer free-space binding energy is well fitted by the effective-range expansion [12]: $E_b(B) = (\hbar^2/\mu r_0^2)(1 - r_0/a(B) - \sqrt{1 - 2r_0/a(B)})$, with $r_0 = 168.37a_0$ for B ranging from 0 to 3.84 mT.

In the experiment, we load a crossed dipole trap, created by two orthogonal, linearly polarized, laser beams ($\lambda = 1064$ nm, waists $\simeq 70$ μm), with a ^{41}K-^{87}Rb mixture in the $|F = 1, m_F = 1\rangle$ hyperfine state, at 1.5 μK. By

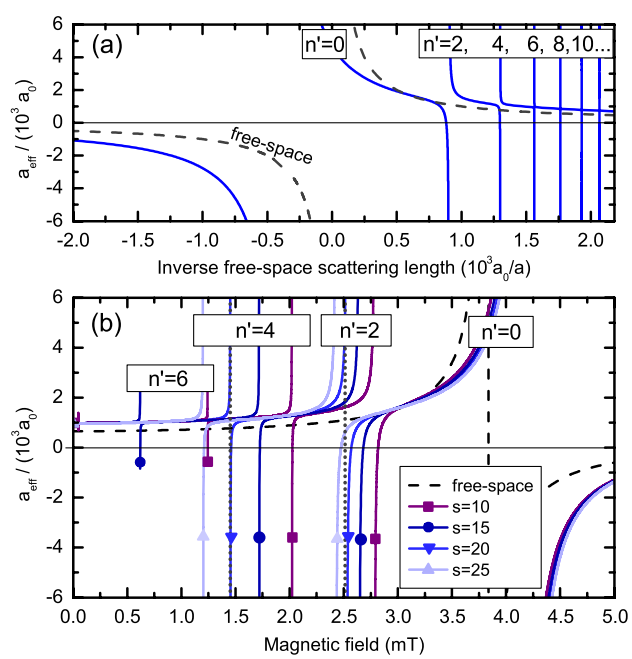

FIG. 2 (color online). (a) Calculated $a_{\rm eff}$ as a function of $1/a$ for the masses of our mixture and $s = 20$. The dashed line corresponds to $a_{\rm eff} = a$. Only even n' resonances are allowed (see text). (b) Calculated $a_{\rm eff}$ as a function of the magnetic field, for several lattice strengths s. The dotted lines show the resonance positions calculated from Eq. (1) for $n' = 2, 4$ and $s = 20$.

lowering the beams intensity, we evaporatively cool the atoms to 0.3 μK in the presence of a uniform field of 7.7 mT for which the interspecies scattering length is convenient ($\sim 260a_0$) to ensure both fast thermalization and a low rate of inelastic collisions. The final temperature is sufficiently high to avoid Bose-Einstein condensation of the samples, but also low enough to make sure that ^{41}K occupies only the ground state of the tight confining potential ($k_B T \ll \hbar\omega$). At this point, we ramp the Feshbach field to 1.4 mT in 20 ms and, immediately afterwards, we raise a 1D SSDP lattice with an exponential ramp of 50 ms (time constant of 10 ms). We then bring the Feshbach field to the final value B in 15 ms and wait typically for 65 ms. We verified that no discernible fraction of ^{41}K atoms lies in excited bands. During the hold time the atom number decays through inelastic 3-body recombination collisions; after the lattice is linearly extinguished in 3 ms and the atoms expand freely for 6 ms, we record the number and temperature of both atomic samples for different values of the final Feshbach field. The presence of the scattering resonance is detected as a pronounced peak in the atom loss due to a resonant enhancement in the 3-body recombination rate.

The SSDP lattice is a standing wave along the horizontal x direction, with linear polarization oriented along the z direction of the Feshbach field and waist equal to 85 μm. The SSDP wavelength $\lambda = 2\pi/k_L = 790.018(2)$ nm is chosen by minimizing the effect of Raman-Nath diffraction on Rb atoms. With respect to our previous work [11], we improved the extinction ratio $V_{\rm lat}^{\rm Rb}/V_{\rm lat}^{\rm K}$ to be lower than 10^{-2} by purifying the lattice polarization.

We observe a quite rich spectrum of inelastic losses with several minima of the total atom number, such that a comprehensive identification of the different peaks requires broad magnetic field scans from approximately 1.5 to 5 mT with a resolution of 7.5 μT (Fig. 3). The first notable feature is that, already for $s = 10$ at the magnetic field of the free-space Feshbach resonance ($B_0 = 3.84$ mT) there is no minimum of atom number. Instead we find a peak of losses at higher magnetic field, around 4.0 mT, where $a < 0$. Several additional minima are found in a magnetic field region where $a > 0$. Position and width of these peaks depend on the lattice strength: as we increase s, the peaks get narrower and shift towards lower B fields, with the exception of the minimum at $B > B_0$ which slightly shifts in the opposite direction. In Fig. 3, we also show the predictions of MDR positions given by the above reported analysis. While the model correctly describes the trends, the agreement with the peak positions is qualitative. In order to make more accurate predictions, we take into account that the lattice actually creates many adjacent wells that can be treated as pure individual 2D traps for ^{41}K only on time scales much shorter than the hopping time between neighboring sites, τ_h. Since in our case τ_h is comparable to the experimental duration, ^{41}K atoms can indeed delocalize over the lattice. As a consequence, we

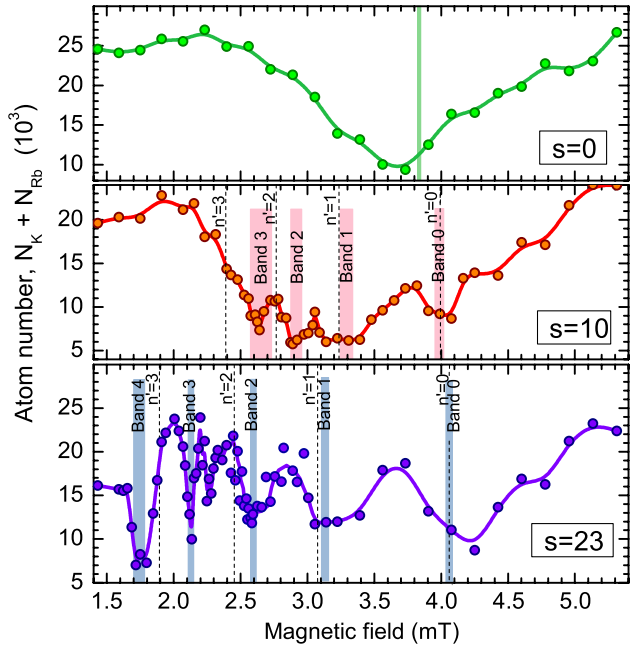

FIG. 3 (color online). Recorded atom number $N_{\rm K} + N_{\rm Rb}$, versus the Feshbach magnetic field without lattice (top), with a SSDP lattice strength $s = 10$ (middle) and $s = 23$ (bottom). Solid lines are a guide to the eye. Predictions based on the harmonic oscillator analysis, Eq. (1) (dashed) and on band structure, Eq. (2) (shaded areas) are shown.

introduce the energy band structure and calculate the positions of the expected resonances by means of

$$p^2/(2m_{\rm Rb}) + \epsilon_{\rm K}(0, q; V_{\rm lat}^{\rm K}) = \epsilon_{\rm KRb}(n', q + p; V_{\rm lat}^{\rm K}) - E_b, \tag{2}$$

where $\epsilon_i(n, q; V_{\rm lat}^{\rm K})$ denotes the energy of the Bloch wave of particle $i(=$ K, KRb), with quasimomentum q in the nth band at the lattice potential $V_{\rm lat}^{\rm K}$, and p the initial momentum of the Rb atom. Like Eq. (1), also Eq. (2) is based on two assumptions. First, the binding energy of the dimer in an excited band equals that in free space, E_b: this assumption is reasonable whenever the dimer size is smaller than the on-site oscillator length ($\hbar/\sqrt{\mu E_b} \ll l_{\rm ho}$), i.e., outside a small region around the free-space resonance. Second, we assume the resonance to occur at the energy crossing, disregarding the shift due to the channel coupling, with the exception of the $n' = 0$ MDR for which we take the same channel-coupling shift as in free space ($b \sim 0.45$ mT). We expect that, in the presence of the lattice, the channel coupling should be smaller than in free space, decreasing as we increase the band index and the lattice strength. As shown in Fig. 4, Eq. (2) predicts the position of the MDRs with improved accuracy with respect to the harmonic oscillator analysis.

In addition, in the case of harmonic confinement, symmetry under parity inversion allows for coupling only between oscillator levels differing by an even number of quanta, at zero collision energy. This is not the case for

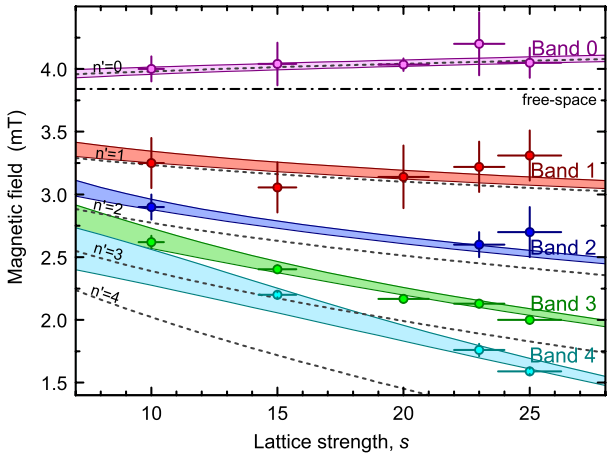

FIG. 4 (color online). Summary of observed loss peak centers as a function of the lattice strength s. Resonance positions are extracted from magnetic field scans (see Fig. 2), by fitting the bottom of the loss peaks with a Gaussian. Error bars are dominated by the width of the loss peaks (vertical) and by the systematic uncertainty in the lattice calibration (horizontal). Predictions based on the harmonic oscillator analysis, Eq. (1) (dashed) and on band structure, Eq. (2) (shaded areas) are shown.

Bloch waves of generic quasimomentum q that are not eigenstates of the parity inversion operator. For nonzero collision energy, i.e., $p_{\mathrm{Rb}} > 0$, coupling to odd n' harmonic oscillator levels is allowed, but suppressed at low temperature. We observe resonances for all indices n', including odd values, with similar strengths. In our case, due to the initial temperature $T = 0.3\ \mu$K, quite a large part of the first Brillouin zone ($|q| < k_L$) is populated by K atoms, since $\sqrt{k_B T m_{\mathrm{K}}}/\hbar \simeq 0.62 k_L$. However, we expect that peaks with odd n' values are observed for sufficiently long hold times even at zero temperature, due to the interaction-induced momentum spread of atoms. For $s = 23$ and 25, we also detect a loss peak located between the $n' = 2$ and $n' = 3$ peaks. At present we cannot explain these features, that might be due to few-body physics.

In conclusion, we have realized a binary system, whose components have different dimensionality, by means of a SSDP lattice that tightly confines only one of them. By monitoring 3-body inelastic losses we have observed for the first time a series of multiple MDRs between (2D) ^{41}K and (3D) ^{87}Rb atoms. Approximating the individual lattice wells as harmonic potentials, a simple argument based on the degeneracy of open and closed channels explains qualitatively the behavior of loss peaks and is consistent with the more complete formal theory. However, the harmonic oscillator analysis must be replaced with band theory to get a quantitative agreement with the peaks location and to explain the presence of odd n' peaks. At present, a comprehensive theory of 3-body inelastic losses for multiple neighboring MDR is still needed.

Besides their specific interest, mix-dimensional configurations are also the extreme case of heteronuclear systems with asymmetric confinement [16], that are frequently encountered in the domain of atomic quantum gases. For weak confinements ($\hbar\omega \ll E_b$) the effect of the potential is negligible and its asymmetry is irrelevant, but for tight confinements, such as those in optical lattice, the scattering modifications need to be taken into account [17], as manifested by our findings. Mix-dimensional atomic systems open many intriguing perspectives: long-lived p-wave trimers close to a MDR [18], a rich Efimov physics [8], and a new kind of heteronuclear molecules, whose constituents live in different dimensions, could be investigated.

This work was supported by MIUR PRIN 2007, Ente CdR in Firenze, CNR under EuroQUAM DQS, EU under STREP CHIMONO and NAME-QUAM, and MIT Department of Physics Pappalardo Program. We thank M. Jona-Lasinio and the QDG group at LENS for fruitful discussions.

Note added in proof.—After submission of this manuscript a new work on CIR in low dimensions has been posted [19].

[1] Z. Hadzibabic *et al.*, Nature (London) **441**, 1118 (2006); V. Schweikhard, S. Tung, and E. A. Cornell, Phys. Rev. Lett. **99**, 030401 (2007); P. Cladé *et al.*, Phys. Rev. Lett. **102**, 170401 (2009).
[2] B. Paredes *et al.*, Nature (London) **429**, 277 (2004); T. Kinoshita, T. Wenger, and D. S. Weiss, Science **305**, 1125 (2004); E. Haller *et al.*, Science **325**, 1224 (2009).
[3] M. Olshanii, Phys. Rev. Lett. **81**, 938 (1998).
[4] T. Bergeman, M. G. Moore, and M. Olshanii, Phys. Rev. Lett. **91**, 163201 (2003).
[5] D. S. Petrov and G. V. Shlyapnikov, Phys. Rev. A **64**, 012706 (2001).
[6] H. Moritz *et al.*, Phys. Rev. Lett. **94**, 210401 (2005).
[7] P. Massignan and Y. Castin, Phys. Rev. A **74**, 013616 (2006).
[8] Y. Nishida and S. Tan, Phys. Rev. Lett. **101**, 170401 (2008).
[9] L. Randall and R. Sundrum, Phys. Rev. Lett. **83**, 3370 (1999).
[10] L. J. LeBlanc and J. H. Thywissen, Phys. Rev. A **75**, 053612 (2007).
[11] J. Catani *et al.*, Phys. Rev. Lett. **103**, 140401 (2009).
[12] D. S. Petrov, Phys. Rev. Lett. **93**, 143201 (2004).
[13] G. Thalhammer *et al.*, Phys. Rev. Lett. **100**, 210402 (2008).
[14] C. Weber *et al.*, Phys. Rev. A **78**, 061601(R) (2008).
[15] G. Thalhammer *et al.*, New J. Phys. **11**, 055044 (2009).
[16] V. Peano, M. Thorwart, C. Mora, and R. Egger, New J. Phys. **7**, 192 (2005).
[17] P. O. Fedichev, M. J. Bijlsma, and P. Zoller, Phys. Rev. Lett. **92**, 080401 (2004).
[18] Y. Nishida and S. Tan, Phys. Rev. A **79**, 060701(R) (2009); J. Levinsen, T. G. Tiecke, J. T. M. Walraven, and D. S. Petrov, Phys. Rev. Lett. **103**, 153202 (2009).
[19] E. Haller *et al.*, arXiv:cond-mat/1002.3795v1.